Front. Optoelectron. 2018, 11(1): 23–29
https://doi.org/10.1007/s12200-018-0759-3

REVIEW ARTICLE

Recent advances in photonic dosimeters for medical radiation therapy

James ARCHER, Enbang LI (✉)

Centre for Medical Radiation Physics, University of Wollongong, Wollongong NSW 2522, Australia

Abstract Radiation therapy, which uses X-rays to destroy or injure cancer cells, has become one of the most important modalities to treat the primary cancer or advanced cancer. High resolution, water equivalent and passive X-ray dosimeters are highly desirable for developing quality assurance (QA) systems for novel cancer therapy like microbeam radiation therapy (MRT) which is currently under development. Here we present the latest developments of high spatial resolution scintillator based photonic dosimeters, and their applications to clinical external radiation beam therapies: specifically high energy linear accelerator (LINAC) photon beams and low energy synchrotron photon beams. We have developed optical fiber dosimeters with spatial resolutions ranging from 50 to 500 μm and tested them with LINAC beams and synchrotron microbeams. For LINAC beams, the fiber-optic probes were exposed to a 6 MV, 10 cm by 10 cm X-ray field and, the beam profiles as well as the depth dose profiles were measured at a source-to-surface distance (SSD) of 100 cm. We have also demonstrated the possibility for temporally separating Cherenkov light from the pulsed LINAC scintillation signals. Using the 50 μm fiber probes, we have successfully resolved the microstructures of the microbeams generated by the imaging and medical beamline (IMBL) at the Australian Synchrotron and measured the peak-to-valley dose ratios (PVDRs). In this paper, we summarize the results we have achieved so far, and discuss the possible solutions to the issues and challenges we have faced, also highlight the future work to further enhance the performances of the photonic dosimeters.

Keywords fiber-optic dosimetry, scintillators, X-ray, Cherenkov radiation, cancer therapy, microbeam radiation therapy (MRT)

Received September 27, 2017; accepted November 24, 2017

E-mail: enbang@uow.edu.au

1 Introduction

Photonic dosimetry is the use of photonic systems to measure radiation dose. There are several mechanisms for generating photons from ionising radiation, the two most widely applied being scintillation light emission and Cherenkov radiation. Originally pioneered by Sir William Crookes in 1903 [1], scintillation detectors have found a wide variety of applications in the century following their discovery. Scintillators are materials that emit visible light upon the absorption with ionising radiation. There are two main types of scintillators: organic (i.e., hydrocarbon) and inorganic.

The light emission process for organic scintillators is caused by the valence electrons in the organic molecules transitioning into higher singlet and triplet states upon the absorption of ionising radiation, and then decaying back into the ground state, emitting photons. The singlet transitions emit scintillation photons very quickly (within nanoseconds), while the triplet transitions are much slower, due to the necessity of a transition from the lowest triplet state to an excited singlet state for photon emission [1]. Inorganic scintillators emit photons via radiation interactions with a crystal electron band structure. Electron-hole pairs are generated between the valence and conduction bands. Direct recombination results in the slow component of scintillation light being emitted, while excitons (bound electron-hole pairs) recombine at impurity sites generating the fast scintillation component [1].

Discovered by Pavel Cherenkov in 1934, Cherenkov radiation is a phenomenon whereby optical light is radiated by charged particles moving though a medium faster than the speed of light in that medium [2]. The Cherenkov radiation is generated in a cone, whose axis is along the direction of the particle's velocity, with angle defined by $\cos\theta = 1/(n\beta)$, where n is the refractive index of the medium and β is the ratio of the particle speed to that of light. The intensity of the Cherenkov radiation is proportional to λ^{-3} and hence dominates in the bluer wavelengths.

Both scintillation light and Cherenkov light can be used for photonic dosimetry, under certain conditions. By collecting the light generated, and measuring with a photodetector, the relative radiation dose can be determined, and then with calibration against a standard device (such as an ionization chamber) the absolute dose can be measured. Scintillator detectors have been used in a wide variety of applications, such as radiation contamination metering [3], neutrino detectors [4], and X-ray imaging [5,6].

The dosimeter designed by Beddar et al. in 1992 is the foundational design that all later probes have built on [7,8]. They used plastic scintillator (a type of organic scintillator where the scintillator molecules are set in a plastic base) cylinder, of length 4 mm and diameter 1 mm, coupled to a fiber optic of the same diameter, to create a dosimetry probe of sensitive volume 3.14 mm^3. The most important results from their design are that the probe is linear, energy independent and water equivalent. By being both linear in light output compared to absorbed energy, and the total photon output being independent of the energy of incident radiation, the dosimeter response scales in proportion to the absorbed dose. Once the dosimeter is calibrated against a standard (an ionization chamber for example), the dosimeter response is easily converted to absorbed dose.

A dosimeter being water equivalent simply means that the materials of the dosimeter interact with ionising radiation the same that water does. As tissue is the material of interest in clinical radiotherapy, where these high spatial resolution dosimeters are applied, the similarities of tissue to water mean that a dosimeter which is water equivalent requires no further calibration to relate the measured dose to the absorbed dose in tissue. As scintillators are water-equivalent in electron and photon radiation beams [9], this is a major advantage of plastic scintillator photonic dosimeters over other dosimeters.

Cherenkov light has been used for dosimetric purposes. Clinical imaging of radiotracers takes advantage of Cherenkov light, and provides a compliment to positron emission tomography imaging [10]. Electron beam relative dosimetry has also been performed using Cherenkov light and showed favorable results [11,12]. However, when a separate light source is being measured (for example in scintillator dosimetry) any Cherenkov light generated will contaminate the light signal intended to be measured. This can negatively affect both the total dose being measured and the spatial resolution of the dosimeter. For these reasons, Cherenkov light is considered a source of noise in scintillator dosimetry, and needs to be accounted for. Cherenkov light is generated in water and plastic. The standard method of Cherenkov removal in the field of scintillator dosimetry, introduced by Beddar et al. [7,8], uses a parallel probe, but without the scintillator, allowing only the Cherenkov light to be detected. This allows the Cherenkov signal to be subtracted from the contaminated scintillator signal. This is accurate only in fields of low dose gradient. Furthermore, an arrayed probe system would require photo-detection for each pair of scintillator and Cherenkov probes, which would quickly grow cumbersome. Alternate methods for Cherenkov removal have been developed, such as optical filtration [13,14], spectral separation [15,16] and temporal filtration [17,18]. An in-depth review on these methods is provided by Beaulieu and Beddar [9].

In this work, we present the development of high spatial resolution scintillator based photonic dosimeters, and their applications to clinical external radiation beam therapies: specifically high energy linear accelerator (LINAC) photon beams and low energy synchrotron photon beams. LINAC beams have macroscopic field sizes of square centimeters, and do not require a very high spatial resolution for accurate dosimetry. The challenging regions to measure dose in are the edges of the field (the penumbra). Ionization chambers are the standard for this type of dosimetry, which provide very accurate dose measurements, but require sensitive calibrations to temperature and pressure. Plastic scintillator dosimeters have been demonstrated to have a very low temperature dependence and no pressure dependence [7].

Synchrotron microbeam radiation therapy (MRT) is a novel type of external beam radiation therapy currently being investigated for its potential applications in treating children with brain tumors. Current therapies risk damage to nervous system development, whereas in MRT the survivability of healthy tissue is much greater [19–22]. MRT uses high flux X-rays of typical mean energy 70 keV, which are spatially fractionated into planes of thickness 50 μm with separation 400 μm. A major challenge of using MRT clinically is the difficulty posed by the need for a high spatial resolution dosimeter to accurately measure the dose deposited across the microbeams. Currently there are two important measurements to be made of the microbeams for quality assurance (QA) purposes: the peak to valley dose ratio (PVDR), and the microbeam widths [23]. Measuring these quantities ensures the dose is being deposited in the correct places, with maximum sparing in the valleys.

Current methods for microbeam QA use radiochromic film, single crystal diamond dosimeters (SCDDs) or silicon strip detectors (SSDs). Film results are water equivalent, but take time to develop and scan, so do not provide real time dosimetry. The spatial resolution of film is also limited by the film grain size, and the microbeam widths fall below the nominal resolution recommendations of most commercial films [24]. SCDDs and SSDs boast a practical resolution for microbeam dosimetry, but lack water equivalence [25–27]. A crystal scintillator dosimeter has been demonstrated, but this device also lacks water equivalence [28]. We believe a photonic dosimeter has the potential to be applied to MRT QA, as the plastic scintillator dosimeters are water equivalent, have the spatial resolution to resolve microbeams, and can provide real time dosimetry.

2 Photonic dosimeter designs and tests

We present photonic dosimeters that use BC-400 plastic scintillator (Saint-Gobain Crystals) coupled to a 1 mm diameter optical fiber (Eska CK-40). To improve light capture the tip of the probe was coated in BC-620 (Saint-Gobain Crystals) reflective TiO_2 paint (a diagram of the probe is shown in Fig. 1). With this design, three probes were made, with differing thicknesses of plastic scintillator. The thickness of the scintillator defines the one-dimensional spatial resolution of the probe. Thicknesses of 100 and 50 μm were used, defining sensitive volumes of 0.079 and 0.039 mm^3 respectively. A 500 μm probe was also fabricated using BC-444 scintillator (with a slower rise time than the BC-400) to test a method for temporal separation of Cherenkov light being developed [30].

The 100 μm probe was tested using a Varian LA1-EX Clinical LINAC (CLINAC), at the Illawarra Cancer Care Centre, Wollongong Hospital, Wollongong, Australia. Two methods for background subtraction were used and tested: a secondary Cherenkov probe, and a temporal processing method being developed. The light was collected with two RCA-4526 photomultiplier tubes (PMTs), and recorded using a Siglent SDS1102CML digital oscilloscope. The sampling was done at 500 MHz, and at 1 GHz for the temporal separation process. The waveform of the light pulses was recorded for the duration of the 3.5 μs CLINAC pulses. To remove noise (from the PMT) in the signal, 128 CLINAC pulses were sampled and averaged on the oscilloscope. To test repeatability four measurements were taken at each position, allowing a 95% confidence interval to be calculated. The CLINAC was configured to pulse 6 MV photons (peak energy 6 MeV, average energy 2 MeV) in a 10 cm × 10 cm field, a typical therapeutic configuration. To assess the accuracy of the scintillator probe, results were compared to a PinPoint N31014 ionization chamber (IC), under identical bam conditions.

The temporal separation method being developed relies on the Cherenkov light being detected before the scintillation signal has saturated. This, in theory, allows the Cherenkov contribution to be characterized and removed from the total signal.

A beam profile was measured at 15 mm depth in Solid Water (Gammex) and a percent depth dose (PDD) was measured at depths varying from surface to 20 cm. The CLINAC beam profile (Fig. 2) and depth dose (Fig. 3) are in close agreement with the ionization chamber data. Important beam qualities can be calculated from the 100 μm probe data, which we compare to expected results. The distance for the field strength to drop from 80% to 20% (the penumbra) was measured with the 100 μm probe as (4.5±0.7) cm for the left side and (5.0±0.7) cm for the right side. For the IC data, the penumbra is expected to be (0.545±0.005) cm. The depth where the maximum dose is deposited (d_{max}) was measured to be (1.2±0.1) cm, which is expected to be 1.41 cm.

The higher resolution 50 μm probe was tested at the Imaging and Medical Beamline (IMBL) at the Australian Synchrotron, Clayton, Australia. The synchrotron X-rays were generated with a 2.0 T wiggler, have a mean energy of 66 keV, and a typical dose rate of 120 Gy/s. A multi-slit collimator (MSC) can be inserted into the broad beam to fractionate the X-rays into microbeams, of width 50 μm and peak-to-peak separation 400 μm.

The optical signal was measured and digitised by a SensL MiniSM Silicon Photomultiplier 10035 (SiPM) connected to a Texas Instruments 64 channel analog front end (AFE0064). The light signal was integrated by the AFE0064 over 200 μs intervals at a frequency of 2 kHz.

The beam profiles were measured by scanning the probe though the microbeams at 0.1 mm/s. The results are compared to a SSD developed by the Centre for Medical Radiation Physics, University of Wollongong, Wollongong, Australia [25,27]. The SSD has the same resolution

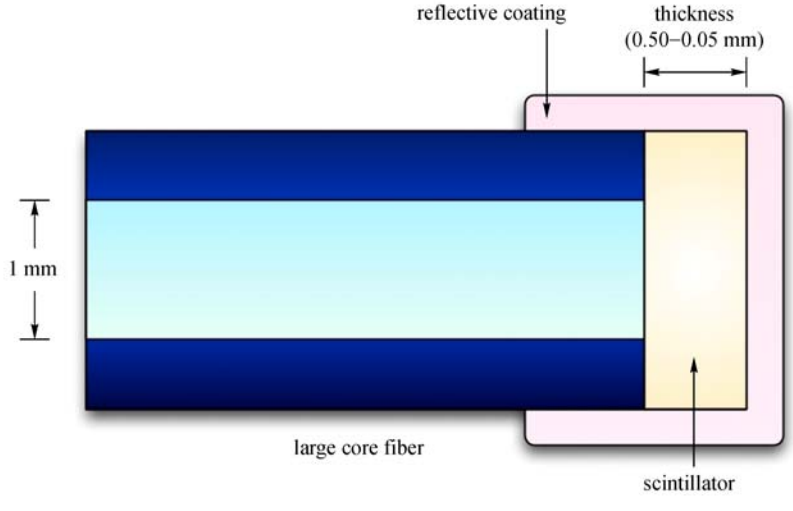

Fig. 1 Diagram of the dosimeter probe. Figure modified from Archer et al. [29]

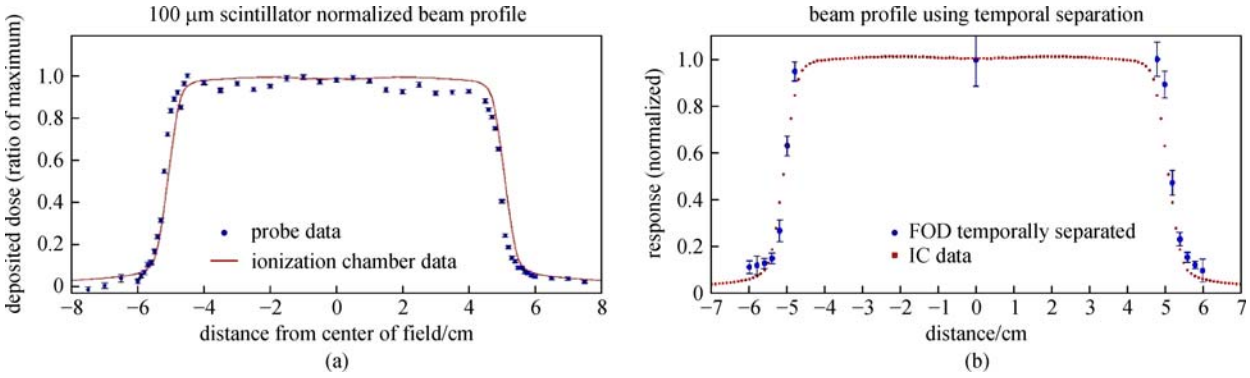

Fig. 2 (a) CLINAC beam profile measured with the fiber optic dosimeter probe (FOD), compared to ionization chamber data. Reproduced from Archer et al. [29]. Temporal separation results are shown in (b)

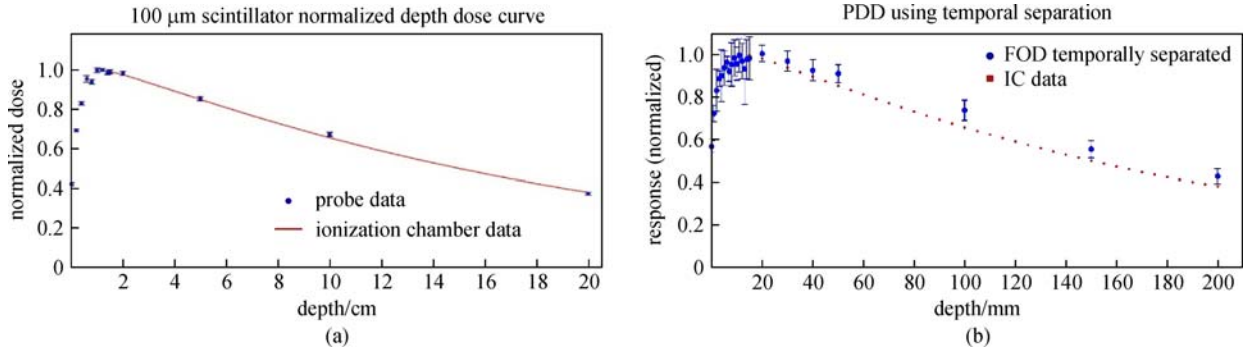

Fig. 3 (a) Percent depth dose of the CLINAC beam measured with the fiber optic dosimeter probe (FOD), compared to ionization chamber data. Reproduced from Archer et al. [29]. Temporal separation results are show in (b)

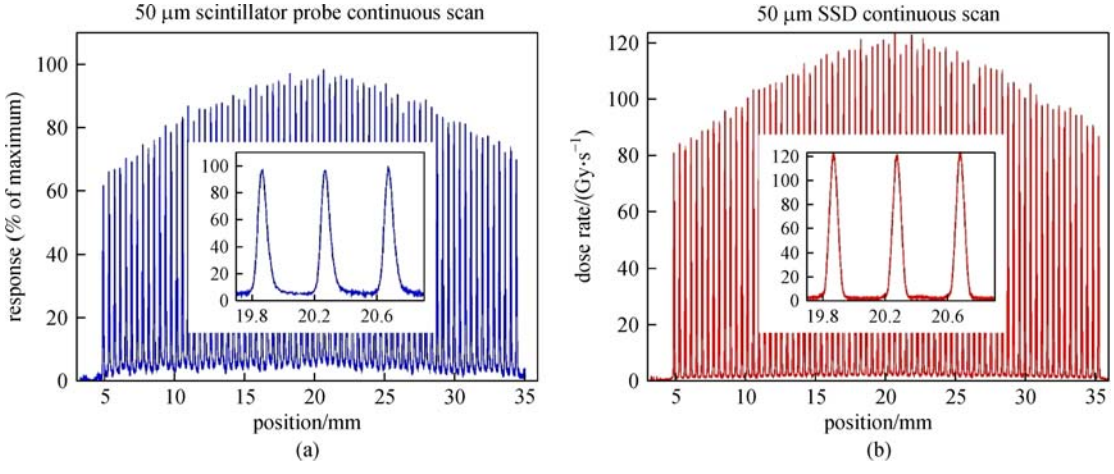

Fig. 4 Microbeam profile measured with (a) 50 μm probe and (b) SSD. Insets show the same three microbeams in closer detail. Reproduced from Archer et al. [31]

(50 μm) as the scintillator probe. The results are shown in Fig. 4. A PDD was also measured in broad beam (without the MSC in place), by scanning the probe through the field at two speeds: 5 and 10 mm/s, and integrating the net signal during the scan. This was compared to a PinPoint N31014 IC, shown in Fig. 5.

The PVDR was measured with the scintillator dosimeter as 19±3 while the SSD measured 26.9±1.4. To assess the resolution of the probe, the full width at half maximum (FWHM) of the measured microbeams was calculated to be (63±3) μm. The FWHM measured with the SSD was (62.4±0.9) μm. This confirms that the scintillator

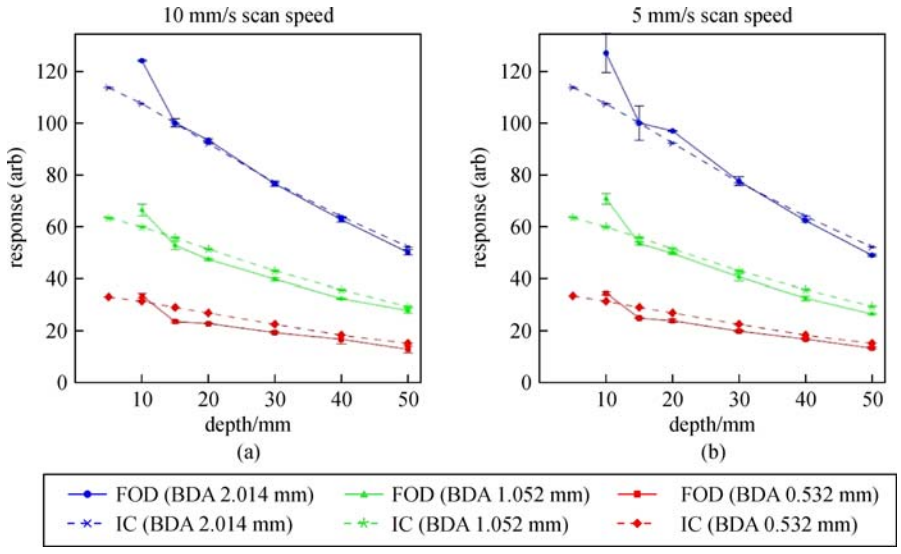

Fig. 5 Percent depth dose plots, measured with the fiber optic dosimeter (FOD) at scanning speeds of (a) 10 mm/s and (b) 5 mm/s. Ionization chamber (IC) results are also shown. Reproduced from Archer et al. [31]

dosimeter and SSD have the same spatial resolution along the direction of the beam. These values are also supported by results derived by convoluting, in one dimension, a rectangular sensitive volume with the intrinsic microbeam field. The intrinsic field was measured using a SCDD with a 1 μm spatial resolution along a single axis (similar to the FOD, in principle) and assumed to match the true field intensity. These results are presented in Fig. 6. The expected FWHM for a 50 μm resolution dosimeter is 57 μm for the measured intrinsic field. The larger values obtained experimentally is due to slight misalignments of the probes to the field.

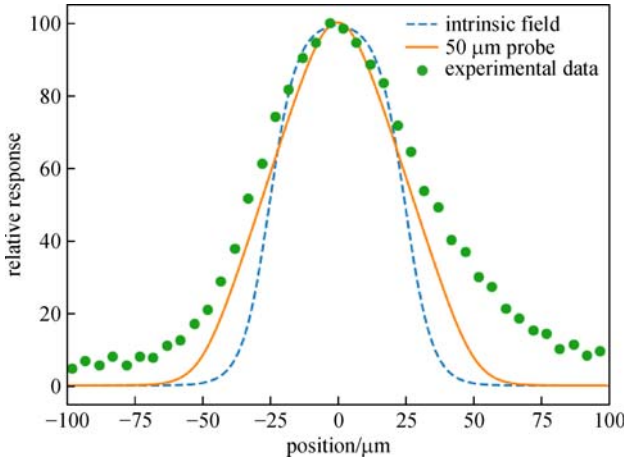

Fig. 6 Intrinsic microbeam field (measures with a 1 μm resolution SCDD) in blue, the convolution of this field with a 50 μm rectangular window in orange, and the experimental data of the central microbeam in green

3 Discussion

There is a general agreement between the scintillator probes and the ionization chamber data. There are several factors that affect the fluctuations and discrepancies that can be seen between the data sets. The ionization chamber results, while measured in the same beam conditions as the FOD data, were not measured at the same time, and so could be responsible in part for discrepancies present. The high voltage supply of the PMT measuring the photon response also drifts throughout the duration of the measurements, altering the gain of the PMTs. This was corrected for using the baseline response outside the field on either side, but fluctuations on a shorter time scale cannot be corrected for using this method. The 500 μm probe results, with the temporal Cherenkov separation algorithm, have much larger uncertainties than the 100 μm probe, despite having the much larger sensitive volume and hence light output. This is due to the separation algorithm being less reliable than the simpler background subtraction, indicating that the method requires more development. The primary difficulty in applying the algorithm is that it assumes the Cherenkov light during the pulse quickly reaches a maximum, and then stays constant for the rest of the pulse. However, measurements of the pure Cherenkov signal indicate that it rises by up to 20% more on a slower time scale. The next steps for this work are to improve the analysis by both adding in extra parameters to fit to the model (such as the tail of the pulse) and to possibly characterize the Cherenkov pulse in more detail with a separate Cherenkov measurement, which can be applied to all subsequent measurements on the same CLINAC machine.

The 100 μm results fluctuate around the expected IC

data. The most significant factor in why this happens is the PMTs gain fluctuating over the approximately hour long data collection. This is the primary reason a SiPM was used for the MRT measurements. The amount of Cherenkov light generated compared to the scintillator light was very high, suggesting that the 100 μm probe is the highest practical resolution achievable for 6 MV photon beams with the photonic dosimeter. This resolution is higher than required, as the highest dose gradient is over a few centimeters, in the penumbra. However for MRT beams, where the photon flux is much higher, and the energies are too low to generate significant Cherenkov light, higher resolutions are practical.

The MRT results in Figs. 4 and 5 are the results of this kind measured with a water equivalent photonic dosimeter. The agreement between the FWHM FOD and SSD results verify the resolution of the probe. The lower PVDR indicates that the valley dose being measured is overestimated, as can be seen in Fig. 4. Figure 5 shows there is a consistent discrepancy between the scintillator probe and IC response at 10 mm depth. Potential explanations include the possible non-water equivalence or energy independence at low energies and unaccounted for nonlinear Cherenkov or fluorescence effects.

The next steps for the high resolution photonic dosimeters for MRT are to test the limits of the spatial resolution achievable with thinner scintillator, and to improve the light collection. A recent experiment has demonstrated the ability of a 20 μm probe to resolve microbeams, and a 10 μm probe is being planned. A study will be done on the optimal combination of scintillator type and photomultiplier, so as to match the scintillation spectrum with the detection efficiency spectrum to get the total photon detection efficiency as best as possible.

The BC-620 paint compromises the water equivalence of the probe, as the titanium atoms have a much higher effective Z number than water. At the thicknesses on the order of hundreds of microns, the paint will scatter the incident radiation more than the plastic, and so will result in both an increase in captured light (the intended effect) as well as an increase in the deposited dose in the scintillator (reducing the water equivalence of the probe). For this reason we intend on investigating the necessity of the paint, as well as alternative, lower Z and much thinner paint or reflective surface options, such as aluminum coating.

4 Conclusion

The results demonstrate, as a proof of concept, the possibility for high spatial resolution photonic dosimeters to be applied to MRT. This is the first water equivalent probe to be applied in this area, due to the significant challenges presented by the low light output of the very small sensitive volume. These results justify the fabrication and testing of even higher resolution probes for this application. The limits of LINAC dosimetry have been reached with the current methods. We have also demonstrated the possibility for temporally separating Cherenkov light from a pulsed LINAC beam, although the algorithm for this required more work to be of a clinical standard.

Acknowledgements This project was supported by UOW's Global Challenges Program. This research was undertaken on the Imaging and Medical beamline at the Australian Synchrotron, Victoria, Australia (AS162/IMBL/10829). This research has been conducted with the support of the Australian Government Research Training Program Scholarship.

References

1. Leo W R. Techniques for Nuclear and Particle Physics. Berlin Heidelberg: Springer, 1994
2. Čerenkov P A. Visible radiation produced by electrons moving in a medium with velocities exceeding that of light. Physical Review, 1937, 52(4): 378–379
3. O'Keeffe S, McCarthy D, Woulfe P, Grattan M W D, Hounsell A R, Sporea D, Mihai L, Vata I, Leen G, Lewis E. A review of recent advances in optical fibre sensors for *in vivo* dosimetry during radiotherapy. The British Journal of Radiology, 2015, 88(1050): 20140702
4. Aberle C, Elagin A, Frisch H J, Wetstein M, Winslow L. Measuring directionality in double-beta decay and neutrino interactions with kiloton-scale scintillation detectors. Journal of Instrumentation, 2014, 9: P06012
5. Rusby D R, Brenner C M, Armstrong C, Wilson L A, Clarke R, Alejo A, Ahmed H, Butler N M H, Haddock D, Higginson A, McClymont A, Mirfayzi S R, Murphy C, Notley M, Oliver P, Allott R, Hernandez-Gomez C, Kar S, McKenna P, Neely D. Pulsed X-ray imaging of high-density objects using a ten picosecond high-intensity laser driver. In: Proceedings of Emerging Imaging & Sensing Technologies. 2016, 9992: 99920E
6. Deas R M, Wilson L A, Rusby D, Alejo A, Allott R, Black P P, Black S E, Borghesi M, Brenner C M, Bryant J, Clarke R J, Collier J C, Edwards B, Foster P, Greenhalgh J, Hernandez-Gomez C, Kar S, Lockley D, Moss R M, Najmudin Z, Pattathil R, Symes D, Whittle M D, Wood J C, McKenna P, Neely D. A laser driven pulsed X-ray backscatter technique for enhanced penetrative imaging. Journal of X-Ray Science and Technology, 2015, 23(6): 791–797
7. Beddar A S, Mackie T R, Attix F H. Water-equivalent plastic scintillation detectors for high-energy beam dosimetry: 1. physical characteristics and theoretical considerations. Physics in Medicine & Biology, 1992, 37(10): 1883–1900
8. Beddar A S, Mackie T R, Attix F H. Water-equivalent plastic scintillation detectors for high-energy beam dosimetry: 2. properties and measurements. Physics in Medicine & Biology, 1992, 37(10): 1901–1913
9. Beaulieu L, Beddar S. Review of plastic and liquid scintillation dosimetry for photon, electron, and proton therapy. Physics in Medicine & Biology, 2016, 61(20): R305
10. Shaffer T M, Pratt E C, Grimm J. Utilizing the power of Cerenkov light with nanotechnology. Nature Nanotechnology, 2017, 12(2):

106

11. Andreozzi J M, Zhang R, Gladstone D J, Williams B B, Glaser A K, Pogue B W, Jarvis L A. Cherenkov imaging method for rapid optimization of clinical treatment geometry in total skin electron beam therapy. Medical Physics, 2016, 43(2): 993–1002
12. Vukolov A V, Novokshonov A I, Potylitsyn A P, Uglov S R. Electron beam diagnostics tool based on Cherenkov radiation in optical fibers. Journal of Physics Conference Series, 2016, 732 (1): 012011
13. Boer S F D, Beddar A S, Rawlinson J A. Optical filtering and spectral measurements of radiation-induced light in plastic scintillation dosimetry. Physics in Medicine & Biology, 1993, 38(7): 945–958
14. Clift M A, Sutton R A, Webb D V. Dealing with Cerenkov radiation generated in organic scintillator dosimeters by bremsstrahlung beams. Physics in Medicine & Biology, 2000, 45(5): 1165–1182
15. Archambault L, Therriault-Proulx F, Beddar S, Beaulieu L. A mathematical formalism for hyperspectral, multipoint plastic scintillation detectors. Physics in Medicine & Biology, 2012, 57 (21): 7133–7145
16. Therriault-Proulx F, Archambault L, Beaulieu L, Beddar S. Development of a novel multi-point plastic scintillation detector with a single optical transmission line for radiation dose measurement. Physics in Medicine & Biology, 2012, 57(21): 7147–7159
17. Clift M A, Johnston P N, Webb D V. A temporal method of avoiding the Cerenkov radiation generated in organic scintillator dosimeters by pulsed mega-voltage electron and photon beams. Physics in Medicine & Biology, 2002, 47(8): 1421–1433
18. Justus B L, Falkenstein P, Huston A L, Plazas M C, Ning H, Miller R W. Gated fiber-optic-coupled detector for *in vivo* real-time radiation dosimetry. Applied Optics, 2004, 43(8): 1663–1668
19. Bouchet A, Lemasson B, Christen T, Potez M, Rome C, Coquery N, Le Clec'h C, Moisan A, Brauer-Krisch E, Leduc G, Remy C, Laissue J A, Barbier E L, Brun E, Serduc R. Synchrotron microbeam radiation therapy induces hypoxia in intracerebral gliosarcoma but not in the normal brain. Radiotherapy and Oncology, 2013, 108(1): 143–148
20. Crosbie J C, Anderson R L, Rothkamm K, Restall C M, Cann L, Ruwanpura S, Meachem S, Yagi N, Svalbe I, Lewis R A, Williams B R, Rogers P A. Tumor cell response to synchrotron microbeam radiation therapy differs markedly from cells in normal tissues. International Journal of Radiation Oncology, Biology, Physics, 2010, 77(3): 886–894
21. Regnard P, Le Duc G, Brauer-Krisch E, Clair C, Kusak A, Dallery D, et al.. Microbeam radiation therapy (MRT) applied to rats´brain tumor: finding the best compromise between normal tissue sparing and tumor curing. European Journal of Cancer Supplements, 2005, 3 (2): 396
22. Serduc R, Vérant P, Vial J C, Farion R, Rocas L, Rémy C, Fadlallah T, Brauer E, Bravin A, Laissue J, Blattmann H, van der Sanden B. *In vivo* two-photon microscopy study of short-term effects of microbeam irradiation on normal mouse brain microvasculature. International Journal of Radiation Oncology, Biology, Physics, 2006, 64(5): 1519–1527
23. Smyth L M L, Senthi S, Crosbie J C, Rogers P A W. The normal tissue effects of microbeam radiotherapy: what do we know, and what do we need to know to plan a human clinical trial? International Journal of Radiation Biology, 2016, 92(6): 302–311
24. Cornelius I, Guatelli S, Fournier P, Crosbie J C, Sanchez Del Rio M, Bräuer-Krisch E, Rosenfeld A, Lerch M. Benchmarking and validation of a Geant4-SHADOW Monte Carlo simulation for dose calculations in microbeam radiation therapy. Journal of Synchrotron Radiation, 2014, 21(3): 518–528
25. Fournier P, Cornelius I, Donzelli M, Requardt H, Nemoz C, Petasecca M, Bräuer-Krisch E, Rosenfeld A, Lerch M. X-Tream quality assurance in synchrotron X-ray microbeam radiation therapy. Journal of Synchrotron Radiation, 2016, 23(5): 1180–1190
26. Fournier P, Cornelius I, Dipuglia A, Cameron M, Davis J A, Cullen A, Petasecca M, Rosenfeld A B, Brauer-Krisch E, Häusermann D, Stevenson A W, Perevertaylo V, Lerch M L F. X-Tream dosimetry of highly brilliant X-ray microbeams in the MRT hutch of the Australian Synchrotron. Radiation Measurements, 2017 doi: 10.1016/j.radmeas.2017.01.011
27. Lerch M L F, Dipuglia A, Cameron M, Fournier P, Davis J, Petasecca M, CorneliusI, PerevertayloV, RosenfeldA B. New 3D silicon detectors for dosimetry in Microbeam Radiation Therapy. Journal of Physics Conference Series, 2017, 777(1): 012009
28. Belley M D, Stanton I N, Hadsell M, Ger R, Langloss B W, Lu J, Zhou O, Chang S X, Therien M J, Yoshizumi T T. Fiber-optic detector for real time dosimetry of a micro-planar X-ray beam. Medical Physics, 2015, 42(4): 1966–1972
29. Archer J, Li E, Petasecca M, Lerch M, Rosenfeld A, Carolan M. High-resolution fiber-optic dosimeters for microbeam radiation therapy. Medical Physics, 2017, 44(5): 1965–1968
30. Archer J, Madden L, Li E, Carolan M, Petasecca M, Metcalfe P, Rosenfeld A. Temporally separating Cherenkov radiation in a scintillator probe exposed to a pulsed X-ray beam. Physica Medica, 2017, 42: 185–188
31. Archer J, Li E, Petasecca M, Dipuglia A, Cameron M, Stevenson A, Hall C, Hausermann D, Rosenfeld A, Lerch M. X-ray microbeam measurements with a high resolution scintillator fibre-optic dosimeter. Scientific Reports, 2017, 7(1): 12450

James Archer received his B.Sc. degree with honours in Physics from the University of Wollongong, Australia, in 2014. He has since been studying as a graduate student at the Centre for Medical Radiation Physics at the University of Wollongong, where he primarily researches fiber optic dosimetry applied to synchrotron X-ray beams.

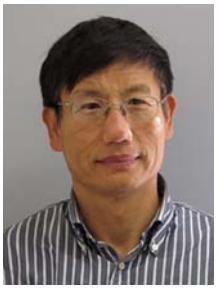

Enbang Li received his B.Sc., Masters and Ph.D. degrees in 1984, 1987 and 1990 respectively from Tianjin University, Tianjin, China. He is currently working at School of Physics, the University of Wollongong, Australia. His research areas include optics and photonics, particularly photonic sensing for biomedical and engineering applications.